

Accuracy of a Non-Smooth Time Stepping Scheme with Non-Rigid Contacts for Ice-Structure Interaction

Marnix van den Berg¹, Raed Lubbad¹, Sveinung Løset¹

¹ Sustainable Arctic Marine and Coastal Technology (SAMCoT), Centre for Research-based Innovation (CRI), Norwegian University of Science and Technology, Trondheim, Norway

ABSTRACT

Discrete element methods enable us to model the interactions between individual ice blocks and the structure of interest. This may give information on relevant processes in ice-structure or ice-ice interaction that cannot be captured by continuous methods. Discrete element methods can broadly be divided into two categories; smooth and non-smooth. While the former is known for high computational cost, the latter may significantly reduce the calculation time of discrete element simulations by enabling larger time steps. This paper investigates the applicability bounds of a novel non-smooth discrete element time stepping scheme that includes contact non-rigidity. Contact non-rigidity allows us to compute ice-structure or ice-ice contact forces based on crushing assumptions. Additionally, it enables the modelling of deformable ice features and failure. A major advantage of the applied method is that it maintains stability for a much wider range of time step sizes. This enables discrete element simulations with a much reduced calculation time compared to smooth methods. The accuracy of the applied method is investigated for two case studies. Results show that accurate results can be generated with significantly larger time steps than used in other methods.

KEY WORDS: Lattice model; Non-Smooth DEM; Ice-Structure interaction

INTRODUCTION

Full-scale ice-structure interaction is of interest in the design of structures and ships, and in the planning of ice management operations. Several numerical approaches are possible to model these interactions. A distinction can be made between continuum methods and discrete methods. The latter models the individual ice blocks as discrete bodies, while continuum methods take the influence of broken ice into account by approximating the bulk material properties of ice and ice rubble. Some phenomena can only be studied using discrete methods, such as the formation of force chains within broken ice. A downside of discrete methods is the computational demand.

Discrete element methods can broadly be divided into two categories; smooth and non-smooth. The difference between smooth and non-smooth discrete element methods can be understood as the difference between explicit and implicit time integration (Servin et al. 2014). Smooth- or explicit methods require only simple evaluations per time step, but need very small time steps to maintain stability. Non-smooth- or implicit methods, on the other hand, require the solution of a system of equations for each time step, but they maintain accuracy for larger time step sizes. The use of non-smooth discrete element methods may significantly reduce the calculation time of discrete ice-structure interaction simulations. A downside of many existing non-smooth discrete element methods is that contacts are assumed infinitely rigid. This makes the contact forces predicted by such methods unphysical for most ice structure interaction scenarios.

This paper presents a novel method that extends the ‘classical’ non-smooth formulation to account for contact non-rigidity. This results in a time stepping scheme that still has all advantages of the non-smooth methods, namely 1) the stability is independent of time step size, 2) it can handle rigid (infinitely stiff) contacts, and 3) it gives accurate results for larger time steps. In addition, the new method is capable of accounting for contact non-rigidity, and it predicts physically correct contact forces. With the proper choice of model parameters, the current scheme can be as accurate as smooth schemes. The time stepping scheme used in this paper differs from schemes published by others (Lacoursiere 2007; Servin et al. 2014; Krabbenhoft et al. 2012) in that it is derived based on the second-order accurate Newmark-Beta method. In contrast to other schemes, it does not introduce (artificial) numerical damping.

Although the proposed method maintains stability for a wide range of time step sizes, the accuracy of the results may be compromised before instability occurs. This paper investigates the influence of time step size, as well as mesh size on the accuracy of the results for two different interaction scenarios; the interaction between a free floating ship and a single square ice floe, and the interaction between a fixed, vertical walled cylindrical structure and a confined floe field.

The paper starts with a short description of the used model. Two case studies are presented. Thereafter, the results are described and discussed. Lastly, the results are summarized and conclusions are drawn.

MODEL DESCRIPTION

The proposed model consists of four parts:

- A *material model*, used to account for the influence of ice floe deformation on the results.
- A *contact model*, used to determine the contact parameters for in ice-ice and ice-structure interactions.
- A *time stepping scheme* used for stable and accurate time integration.
- A *hydrodynamic model*, which accounts for hydrostatic forces, form drag and skin friction.

Ice failure (except local crushing) is not taken into account in the model and results presented in this paper. Therefore, the results should be seen as describing trends in the contact behavior, and should not be perceived as loads that would occur in actual full-scale interaction.

Material Model

A random lattice model based on Voronoi Tessellation is used as a material model for the ice. This model is presented in (van den Berg 2016). The model parameters are determined as described in (Yip et al. 2005) and are adapted to ice plates as described in (van den Berg 2016). Lattice models based on Voronoi tessellation give accurate results in fracture modelling of brittle, inhomogeneous, and/or polycrystalline materials such as concrete and rock.

Contact Model

The contact model is used to derive contact parameters in ice-ice and ice-structure contacts. The model is based on the assumption that local crushing will occur at ice-ice or ice-structure contacts when a maximum crushing pressure is exceeded. Full-scale observations show that local crushing does indeed occur in most ice-ice and ice-structure interactions. An example of local crushing is shown in Figure 1.

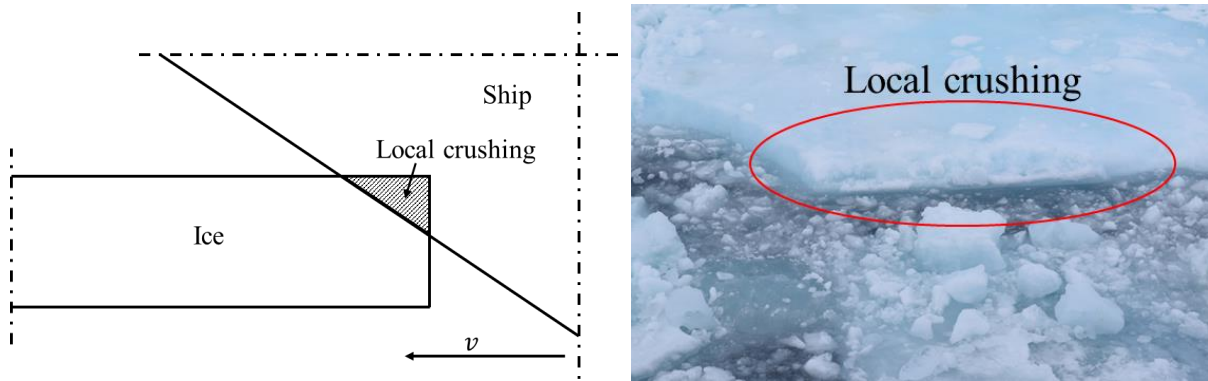


Figure 1. Local crushing at ship-ice contact. Sketch of interaction scenario (left) and full-scale observation (right, Oden 2016).

We find that it is essential to take this local crushing into account for an accurate contact force determination. The contact parameters are determined assuming constant energy dissipation per crushed volume. This is similar to (Kinnunen et al. 2016) and is supported by experiments described in (Kim & Høyland 2014). We note that the assumption of a constant energy absorption during crushing is a simplification of the actual phenomena that occur during crushing. Such a simplification is needed because of the large difference in scale between the phenomena that occur at the ice-structure contact and the global ice sheet behavior. To our knowledge, a similar simplification is made in any global ice structure interaction model, the only difference being the assumptions made in deriving the force-penetration curve. Models that attempt to physically model the crushing process are currently limited to small scales.

We derive an expression for the contact force as a function of penetration in the form:

$$F(\delta) = p_{cr1}\delta^2 + p_{cr2}\delta + p_{cr3} \quad (1)$$

In which the constants p_{cr1} , p_{cr2} and p_{cr3} are determined based on the contact geometry and the specific energy absorption during crushing. F is the contact force in the normal direction of the contact and δ is the crushing penetration in the normal direction. Crushing contacts are fully dissipative; the energy ‘consumed’ in the crushing process cannot be recovered.

Time Stepping Scheme

The time stepping scheme utilizes the contact parameters derived from the lattice model and the contact model to propagate the simulation in an implicit manner. The time stepping scheme used for the simulations in this paper is a relatively new way of modelling, and shows similarities with the methods described in (Lacoursiere 2007; Servin et al. 2014; Krabbenhoft et al. 2012). However, the derivation of the current method is based on a different implicit integration method, resulting in different integration factors and model properties. It is derived based on the second-order accurate Newmark-Beta method. In contrast to other schemes, it does not introduce (artificial) numerical damping.

Each time step, the velocity change of the bodies $\Delta \mathbf{v}$ and the contact force integral at each contact λ is calculated by solving the system of equations shown in formula 2:

$$\begin{bmatrix} \mathbf{M} & -\mathbf{J}^T \\ -\mathbf{J} & \mathbf{\Sigma} \end{bmatrix} \begin{bmatrix} \Delta \mathbf{v} \\ \lambda \end{bmatrix} = \begin{bmatrix} \mathbf{0} \\ \mathbf{G} \end{bmatrix} \quad (2)$$

Here, \mathbf{M} is the mass matrix, \mathbf{J} is a matrix containing the constraint Jacobians, $\Delta \mathbf{v}$ contains the velocity change of each body and λ are the Lagrange multipliers at each contact, which have the dimension of impulse in this formulation. The diagonal matrices $\mathbf{\Sigma}$ and \mathbf{G} describe the contact non-rigidity. The terms in $\mathbf{\Sigma}$ and \mathbf{G} are derived by ensuring energy balance at each contact and utilizing an implicit integration scheme similar to the Newmark-Beta method. The terms in $\mathbf{\Sigma}$ and \mathbf{G} can be used to represent elastic contacts, like the lattice elements representing the ice deformation, or they can represent dissipative contacts for contact between separate ice floes or between ice and structure, in which local crushing occurs.

At ice-ice or ice-structure contacts, there cannot be any tension and the frictional force is limited based on the normal force. Coulomb friction is assumed, resulting in the following constraints for loose contacts;

$$\lambda_n \geq 0 \quad (\text{no tension}) \quad (3)$$

$$\lambda_{t,i} \leq \mu \lambda_{n,i} \quad (4)$$

In which μ is the friction coefficient. λ_n is the integral of normal force over the time step and λ_t is the integral of frictional forces over a time step;

$$\lambda_n = \int_{t_n}^{t_{n+1}} F_n(t) dt \quad (5)$$

$$\lambda_t = \int_{t_n}^{t_{n+1}} F_t(t) dt \quad (6)$$

Hydrodynamic Model

Hydrodynamic drag and hydrostatic forces are included in the model. The drag is calculated based on a quadratic drag equation and skin friction. More details can be found in (Tsarau 2015). The effect of added mass is not taken into account. This may influence the results at higher interaction velocities.

DESCRIPTION OF CASE STUDIES

We investigate the influence of time step, mesh size and interaction velocity on the contact force, contact area and sheet deformation in the time domain. The influence of these parameters is investigated for two cases:

- Case #1: Interaction between a ship-shaped structure (sloping at the waterline) and a single 100x100 m ice floe.
- Case #2: Interaction between a bottom-fixed circular-shaped structure (vertical at the waterline) and a confined floe field of 100 x 100 m. The floes are randomly generated according to the method described in (Yulmetov et al. 2014) and have areas between 100 and 400 m².

Figure 2 and Figure 3 show the two case studies. In Case #1, a ship interacts with a free-floating ice floe. In the initial condition, the ice has no velocity and the ship propagates in the direction indicated in the figure. The velocity of the ship is not constant, as it interacts with the ice, the ship slows down and the ice floe accelerates.

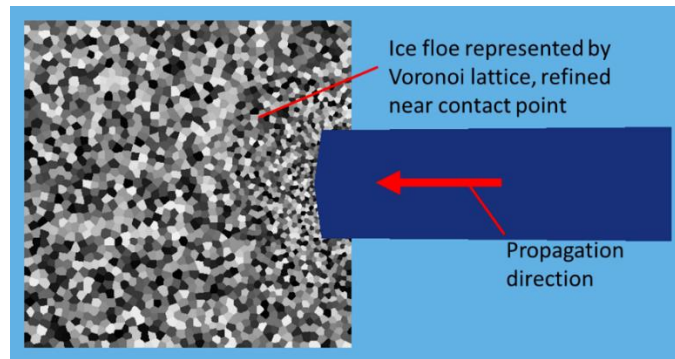


Figure 2. Ship-ice interaction scenario, top view.

In Case #2, the ice floes are confined by the domain boundaries, as they would be in an ice tank. In full-scale, the confinement could come from larger ice floes or ice pressure situations. The cylindrical structure is propagated with a constant velocity of 2.0 m/s in the direction indicated in the figure.

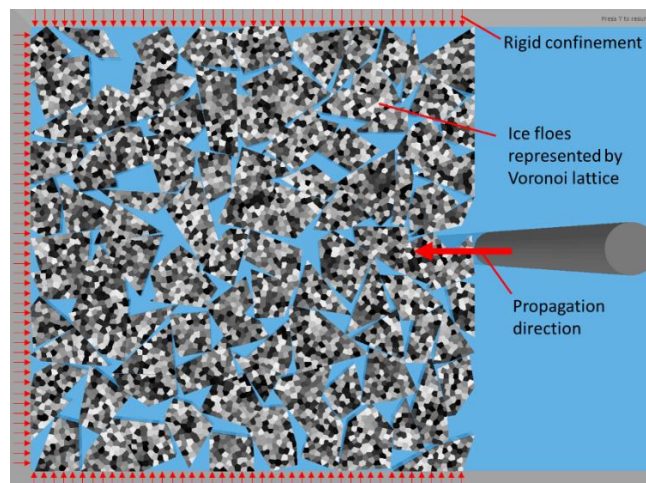


Figure 3. Fixed structure interaction scenario, top view.

Other simulation parameters are shown in Table 1.

Table 1. Simulation parameters

Parameter	Value
Ice thickness	1.0 m
Time step	variable, see Table 2
Ice-structure friction coefficient	0.3
Water density	1025 kg/m ³
Ice density	910 kg/m ³
Young's modulus of ice	5.0 · 10 ⁹ N/m ²
Poisson's ratio*	0
Specific energy absorption during crushing**	2.0 · 10 ⁶ J/m ³
Mesh size	variable, see Table 2
Interaction velocity	variable, see Table 2

* The current method of lattice properties determination does not allow for accurate modelling of Poisson effects. Therefore, a value of 0 is used.

** This corresponds to a constant crushing pressure of 2.0 MPa.

The ship dimensions are roughly similar to that of existing icebreakers, however it does not match any existing icebreaker in particular. The ship has a stem angle of 33.7°. The middle of the ship bow protrudes compared to the sides of the bow. This ensures initial point contact between the ship hull and the ice, which makes the analysis of contact model behavior and sheet deformation more convenient. The diameter of the fixed cylindrical structure matches the diameter of the Nordstrømsgrund lighthouse. The geometry of the ship and the fixed structure are shown in Figure 4.

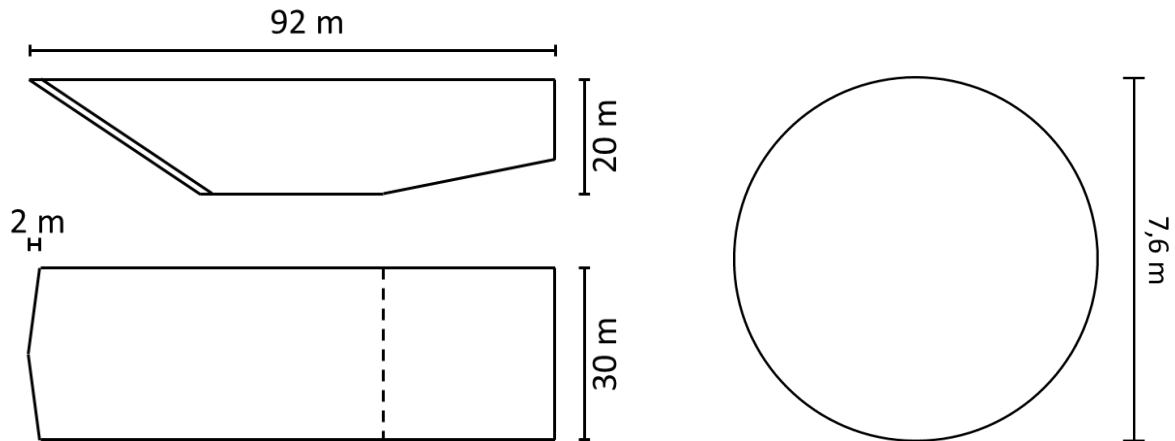


Figure 4. Geometry of ship and fixed cylindrical structure.

RESULTS

In all ice-structure interaction simulations presented below, the following phenomena occur:

- Ice and structure come in contact. Because of roughness of the ice surface area and/or the contact geometry, the contacting area at initial contact between the ice and the structure is close to zero.
- Local crushing occurs at the ice-structure contact, which results in a higher contact area. This higher contact area is needed to transfer a load from the structure to the ice.
- As the contact area and the total contact force between ice and structure increases, the ice sheet starts to deform. This deformation influences the temporal evolution of the contact force.

We consider the above described phenomena a reasonably good approximation of the phenomena that occur during actual ice-structure interaction. During the simulations, the stress distributions in the ice were similar to those displayed in Figure 5. Bending waves were observed in Case #1 (the ship interaction scenario) and force chains formed in Case #2 (the fixed structure scenario).

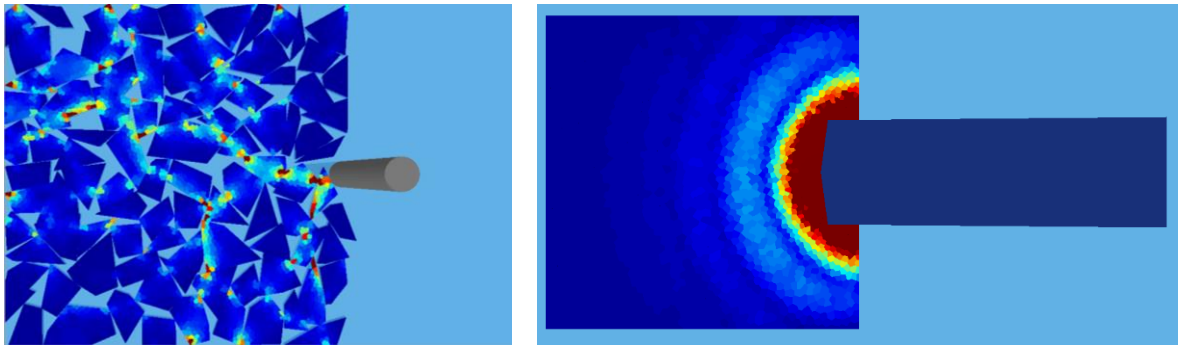


Figure 5. Stress in ice sheets during interaction with fixed structure and ship

We investigate the effect of mesh size (d_s), time step (dt), and interaction velocity (v) on the results of Case #1. For Case #2, we study the effect of mesh size and time step on the results. The combinations of the tested parameters are shown in Table 2.

Table 2. Numerical test matrix

Case number #	Time step (dt) [s]	Mesh size (d_s) [m]	Interaction velocity (v) [m/s]	Structure type
1.1	$1.0 \cdot 10^{-4}$, $5.0 \cdot 10^{-4}$, $1.0 \cdot 10^{-3}$, $5.0 \cdot 10^{-3}$, $1.0 \cdot 10^{-2}$, $5.0 \cdot 10^{-2}$, $1.0 \cdot 10^{-1}$	$[0.5 / 2.0]^*$	5.0	Ship-shaped floater
1.2	$1.0 \cdot 10^{-4}$	$[0.5 / 2.0]$, $[1.0 / 4.0]$, $[1.5 / 6.0]$, $[2.0 / 8.0]$, $[2.5 / 10.0]$, $[3.0 / 12.0]$, $[3.5 / 14.0]^*$	5.0	Ship-shaped floater
1.3	$1.0 \cdot 10^{-2}$	$[0.5 / 2.0]^*$	0.05, 0.1, 0.5, 1.0, 5.0	Ship-shaped floater
2.1	$1.0 \cdot 10^{-3}$, $5.0 \cdot 10^{-3}$, $1.0 \cdot 10^{-2}$, $5.0 \cdot 10^{-2}$, $1.0 \cdot 10^{-1}$	1.0	2.0	Fixed cylindrical
2.2	$1 \cdot 10^{-2}$ s	1.0, 2.0, 5.0, 10.0, ∞	2.0	Fixed cylindrical

* $[d_{smin} / d_{smax}]$ The mesh changes from fine near the contact to a coarser mesh further away.

In the following sections, selected results are presented. First, we present the results for ship-ice interaction. Then we present the results for the fixed structure scenario.

Case #1.1; Influence of Rime Step in Ship-Ice Interaction

In the ship simulation case, the influence of time step size on the results is minimal for $dt \leq 0.01$ s, and is significant for the presented higher step sizes. The results are shown in Figure 6. An interesting observation in the below figures is that while the contact force is lower at $t = 0.1$ s for the large time step cases, the vertical sheet deformation at the contact point is higher at this time. This indicates that the sheet dynamics are no longer accurate at these time steps.

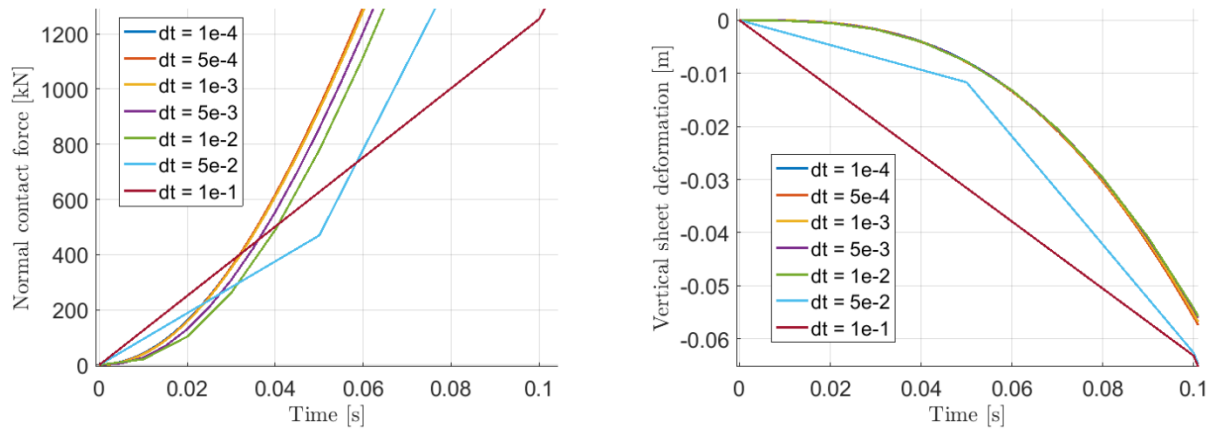


Figure 6. Contact force as a function of time (left) and vertical sheet deformation as a function of time (right), for a range of time step sizes dt .

Case #1.2; Influence of Mesh Size on Ship-Ice Interaction

The influence of mesh size on the contact force and the sheet deformation is shown in Figure 7. Note that the contact force is hardly effected by the mesh size in this simulation case. This may be explained by the result presented in Figure 9. At an interaction velocity $v = 5.0$ m/s, bending deformation is much smaller than the local crushing deformation. This reduces the effect of sheet deformation on contact force. Therefore, the inaccuracy in sheet deformation behavior that occurs for coarser meshes has little effect on the contact force build up. The right plot of Figure 7 shows that the local mesh deformation stiffness is increased as the mesh size increases. This is in line with the results presented in (ref ATC 2016) and can be attributed to the inability of coarse meshes to capture the local sheet deformation near the contact point.

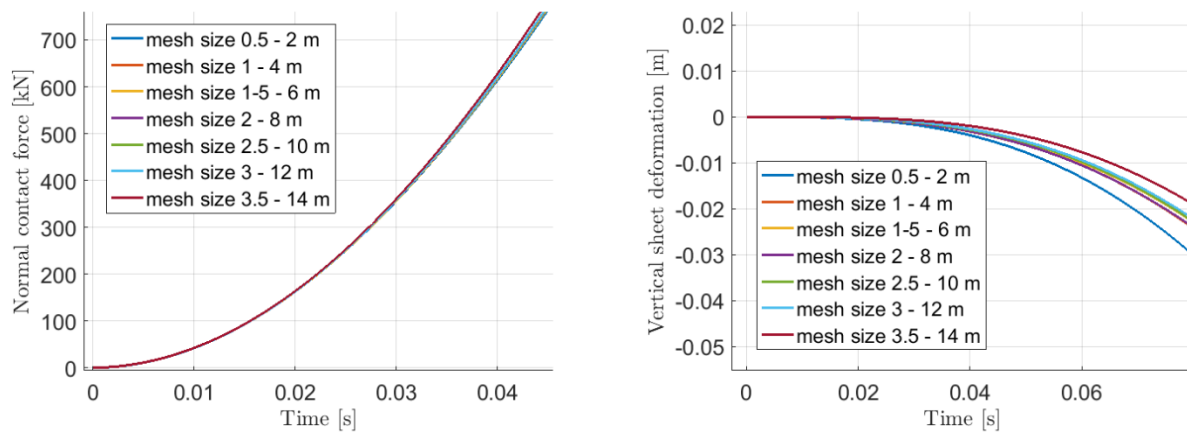


Figure 7. Contact force as a function of time (left) and vertical sheet deformation as a function of time (right), for a range of time step sizes.

Case #1.3; Influence of Interaction Velocity in Ship-Ice Interaction

In contrast to mesh size and time step, which are purely numerical features, the interaction velocity is a parameter of the actual interaction. We choose to investigate and demonstrate the influence of interaction velocity on the model results because it demonstrates the importance of sheet dynamics on the results. The influence of interaction velocity is apparent in Figure 8. Here, the vertical sheet deformation at the loading point is plotted against the contact normal force. At higher interaction velocities, the sheet deformation increases much slower with an increasing normal force. This can be attributed to ice sheet inertia and hydrodynamic damping. Since strain is often used as a failure criterion, different deformation behavior will also result in a different failure pattern. In case of bending failure, this will most likely mean a shorter failure length.

Note that the contact normal force is limited for the lowest interaction velocities, 0.05 m/s and 0.1 m/s. At these velocities, the sheet reaches the same velocity as the ship before the cut-off normal force is reached.

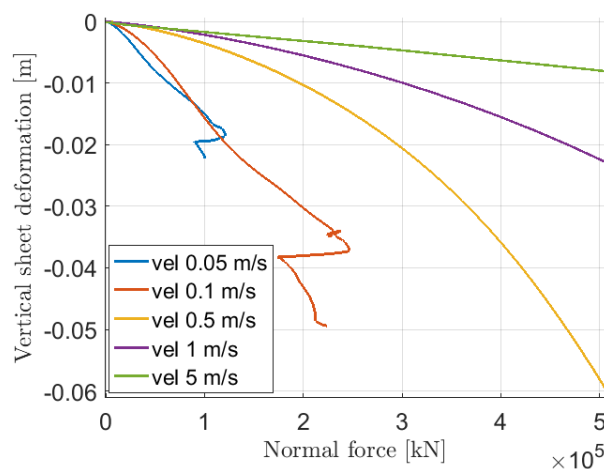


Figure 8. Contact force against sheet deformation for different interaction velocities

Another interesting observation can be made when looking at the difference between local crushing deformation and sheet bending deformation. This is shown in Figure 9. At lower interaction velocities, there is both bending deformation in the ice sheet and local crushing deformation. At high interaction velocities, the sheet deformation is much smaller compared to the crushing deformation, which may result in a steeper increase of the contact force.

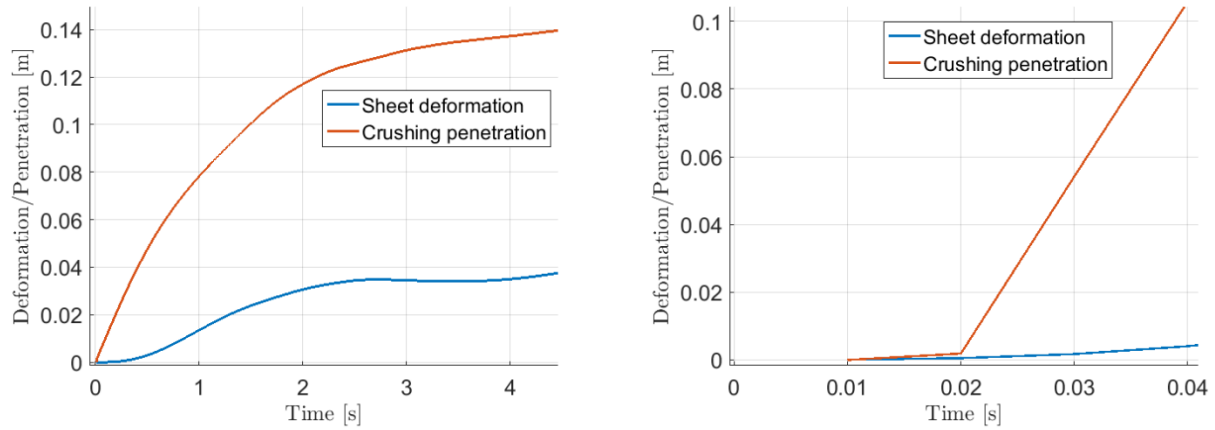


Figure 9. Sheet deformation and crushing penetration at an interaction velocity of 0.1 m/s (left) and 5.0 m/s (right).

Case #2.1; Influence of Time Step on Fixed Structure – Ice Interaction

Figure 10 and Figure 11 shows the load from the ice on the fixed structure in the direction opposite to the propagation direction. Any change in time step causes a clear difference in the load signal. We may wonder if a complete correlation between load-time signals should be expected. Due to the nature of the modelled case, the load at any moment in time depends on the ice floe displacements in the previous simulation steps. Because of this, minimal (numerical) differences in the beginning of the simulation may lead to a completely different load signal later in the simulation. Therefore, the properties of the signals over the duration of the simulation should be compared, rather than comparing the exact load values at any moment in time. The current simulations are considered too short to say anything statistically significant about the load-time signals, but from visual comparison we conclude that the signals for time steps $5.0 \cdot 10^{-2}$ s to $1.0 \cdot 10^{-3}$ s show similar behavior. Even the load-time signal for $1.0 \cdot 10^{-1}$ s has peak loads and an average load value of comparable size.

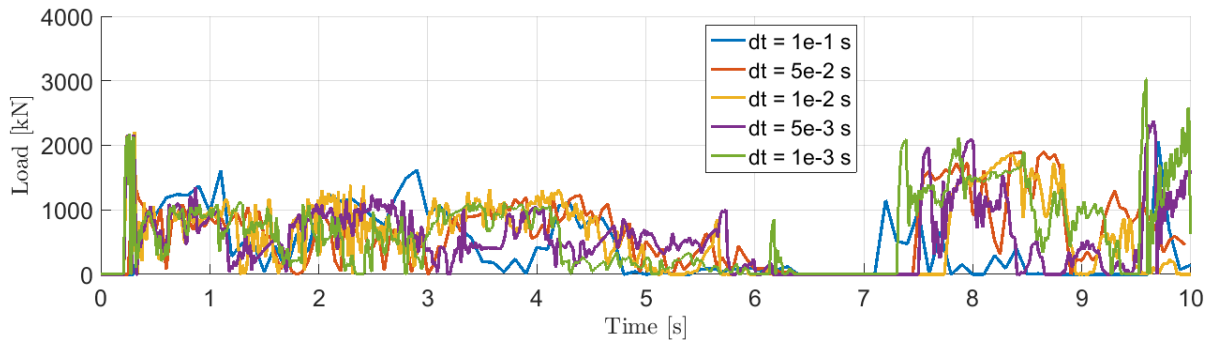


Figure 10. Unfiltered load-time signals, time steps $1 \cdot 10^{-3}$ s to $1 \cdot 10^{-1}$ s.

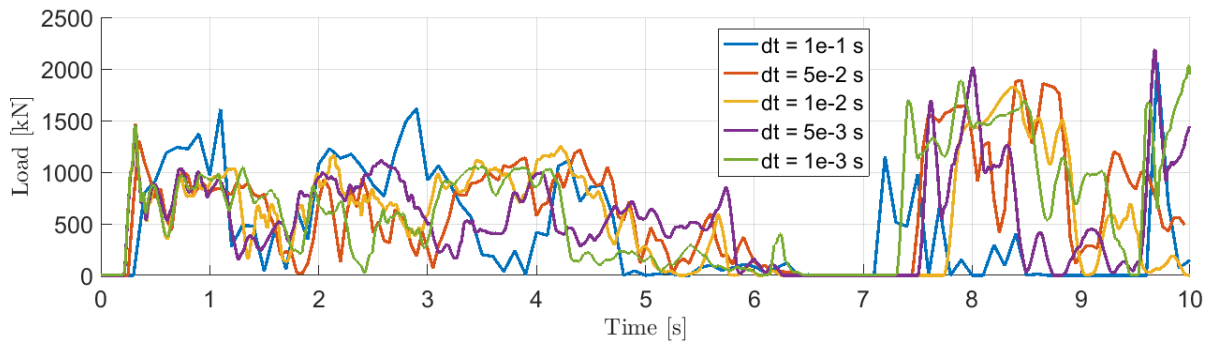


Figure 11. Filtered load-time signals, time steps $1 \cdot 10^{-3} \text{ s}$ to $1 \cdot 10^{-1} \text{ s}$.

Case #2.2; Influence of Mesh Size on Fixed Structure – Ice Interaction

Figure 12 and Figure 13 shows the load from the ice on the fixed structure in propagation direction, in a comparison for different mesh sizes. As discussed in the previous section, we should not expect a correlation over the whole time signal because of the nonlinear nature of the simulation. The results are similar for the first second of the simulation, after which the results start to differ. Comparing the load-time signals over the complete duration, we see that the signals for mesh sizes 5.0 – 1.0 m have broadly similar characteristics. The load-time signals for no mesh and for a mesh size of 10.0 m are similar to each other, but are different from the signals obtained with finer mesh sizes.

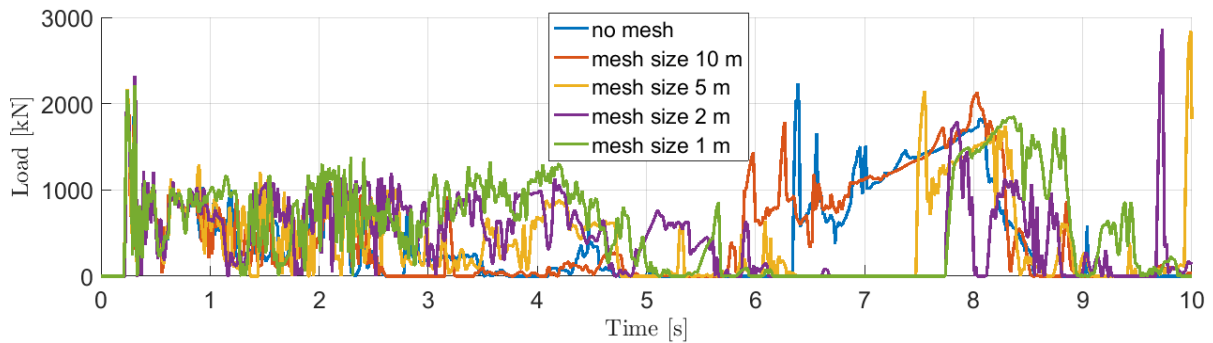


Figure 12. Unfiltered load-time signals, no mesh to mesh size 1 m.

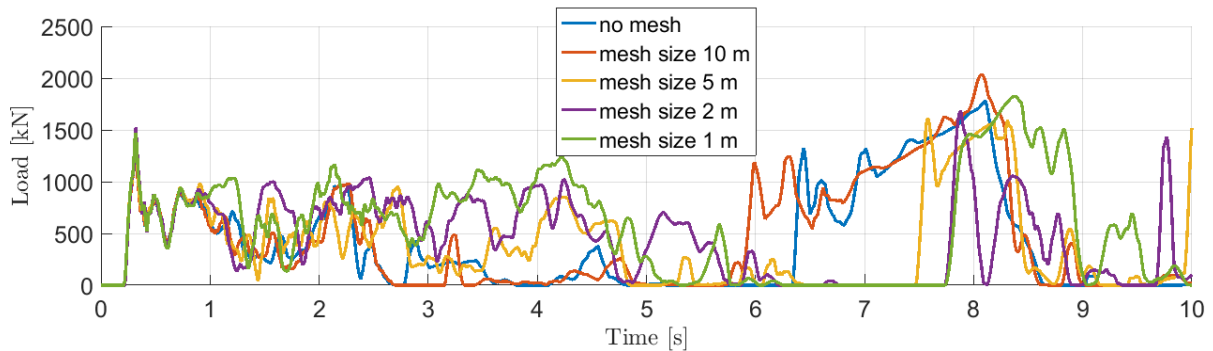


Figure 13. Filtered load-time signals, no mesh to mesh size 1 m.

CONCLUSIONS

The accuracy limits of a novel non-smooth discrete element time stepping scheme that includes contact non-rigidity were investigated. The sensitivity of model results to mesh density, time step and interaction velocity were compared. Based on the results of this analysis, we draw the following conclusions:

Case #1: Ship – Single Floe Interaction

- The ship-ice interaction results can be considered accurate for time steps ≤ 0.01 s. For larger time steps, the model results start to differ significantly.
- The mesh size has little influence on the results in the performed simulations. This is due to the high interaction velocity, which reduces the effect of ice floe deformation on the results.
- At low velocity interaction, the ice floe deformation was significant compared to the local crushing deformation. For high interaction velocities, (> 1 m/s) the sheet deformation is much smaller than the local crushing deformation. Hydrodynamic damping and inertia of the ice floe cause the difference in deformation behavior. This will most likely result in a different failure pattern for high velocity interactions.

Case #2: Fixed Structure Floe Field Interaction

- Due to the nonlinear nature of the simulation, we should not expect a correlation between results over the full time signal. A minimal (numerical) difference in the beginning of the simulation may lead to completely different results later on.
- Comparing the load-time signals for different time step sizes, we find broadly similar results for time steps $5.0 \cdot 10^{-2}$ s to $1.0 \cdot 10^{-3}$ s.
- Comparing the load-time signals for different mesh sizes, the results for mesh sizes 5.0 -1.0 m are broadly similar.

In the fixed structure simulation case #2, the local crushing at ice-ice and ice structure contacts is important for a correct contact force prediction, but the elastic ice floe deformation (taken into account by the lattice model) does not have much influence on the load signal. In the ship simulation case #1, the bending deformation of the ice floe influences the contact force at low interaction velocities. At higher interaction velocities, local crushing is much more important. Since the sheet deformation as a function of contact force is different at high ice velocities, we expect that the failure pattern will also change as a function of interaction velocities. These results were obtained while neglecting the added mass of the water. Including added mass will most likely exacerbate the velocity effects.

ACKNOWLEDGEMENTS

The authors would like to acknowledge the support from the SAMCoT CRI through the Research Council of Norway and all of the SAMCoT Partners.

REFERENCES

- van den Berg, M., 2016. A 3-D Random Lattice Model of Sea Ice. In *Arctic Technology Conference. St. Johns, Newfoundland and Labrador*.
- Kim, E. & Høyland, K. V., 2014. Experimental Investigations of the Energy Absorption Capacity of Ice During Crushing: Is the Specific Energy Scale Independent? *Proceedings of the 22nd IAHR International Symposium on Ice*, pp.163–170.
- Kinnunen, A., Tikanmäki, M. & Heinonen, J., 2016. An energy model for ice crushing in ice-structure impact. In *23 r d IAHR International Symposium on Ice*. Ann Arbor, Michigan, USA, pp. 1–8.
- Krabbenhoft, K. et al., 2012. Granular contact dynamics with particle elasticity. *Granular Matter*, 14(5), pp.607–619.
- Lacoursiere, C., 2007. *Ghosts and machines: regularized variational methods for interactive simulations of multibodies with dry frictional contacts*. Umeå University.
- Servin, M. et al., 2014. Examining the smooth and nonsmooth discrete element approaches to granular matter. *International Journal for Numerical Methods in Engineering*, (March), pp.1885–1891.
- Tsarau, A., 2015. *Numerical Modelling of the Hydrodynamic Effects of Marine Operations in Broken Ice*. Norwegian University of Science and Technology.
- Yip, M., Mohle, J. & Bolander, J.E., 2005. Automated Modeling of Three-Dimensional Structural Components Using Irregular Lattices. *Computer-Aided Civil and Infrastructure Engineering*, 20, pp.393–407.
- Yulmetov, R., Løset, S. & Lubbad, R., 2014. An Effective Numerical Method for Generation of Broken Ice Fields, Consisting of a Large Number of Polygon-Shaped Distinct Floes. In *Proceedings of the 22nd IAHR International Symposium on Ice*.